The EMBO Journal (2010) 29, 222–235 | © 2010 European Molecular Biology Organization | All Rights Reserved 0261-4189/10
www.embojournal.org

THE EMBO JOURNAL

Combinations of genetic mutations in the adult neural stem cell compartment determine brain tumour phenotypes

Thomas S Jacques[1], Alexander Swales[2], Monika J Brzozowski[3,5], Nico V Henriquez[3], Jacqueline M Linehan[2], Zaman Mirzadeh[4], Catherine O' Malley[2], Heike Naumann[2,6], Arturo Alvarez-Buylla[4] and Sebastian Brandner[3,*]

[1]Neural Development Unit, UCL-Institute of Child Health and Department of Histopathology, Great Ormond Street Hospital, London, UK, [2]Department of Neurodegenerative Disease and MRC Prion Unit, UCL Institute of Neurology, London, UK, [3]Division of Neuropathology and Department of Neurodegenerative Disease, UCL Institute of Neurology, London, UK and [4]Department of Neurosurgery and Developmental and Stem Cell Biology Program, University of California, San Francisco, CA, USA

It has been suggested that intrinsic brain tumours originate from a neural stem/progenitor cell population in the subventricular zone of the post-natal brain. However, the influence of the initial genetic mutation on the phenotype as well as the contribution of mature astrocytes to the formation of brain tumours is still not understood. We deleted Rb/p53, Rb/p53/PTEN or PTEN/p53 in adult subventricular stem cells; in ectopically neurografted stem cells; in mature parenchymal astrocytes and in transplanted astrocytes. We found that only stem cells, but not astrocytes, gave rise to brain tumours, independent of their location. This suggests a cell autonomous mechanism that enables stem cells to generate brain tumours, whereas mature astrocytes do not form brain tumours in adults. Recombination of PTEN/p53 gave rise to gliomas whereas deletion of Rb/p53 or Rb/p53/PTEN generated primitive neuroectodermal tumours (PNET), indicating an important role of an initial Rb loss in driving the PNET phenotype. Our study underlines an important role of stem cells and the relevance of initial genetic mutations in the pathogenesis and phenotype of brain tumours.

The EMBO Journal (2010) **29,** 222–235. doi:10.1038/emboj.2009.327; Published online 19 November 2009
Subject Categories: neuroscience; molecular biology of disease
Keywords: brain tumour; soil and seed; stem cells; subventricular zone; tumour suppressor gene

*Corresponding author. Division of Neuropathology, Department of Neurodegenerative Disease, UCL Institute of Neurology, Queen Square, London WC1N 3BG, UK. Tel.: +44 20 7676 2188;
Fax: +44 20 7676 2157; E-mail: s.brandner@ion.ucl.ac.uk
[5]Present address: Proximagen Limited, Hodgkin Building, King's College London, Guy's Campus, London SE1 1UL, UK
[6]Present address: Max-Delbruck Centre, AG Spagnoli, Robert Roessle Str. 10, Berlin 13125, Germany

Received: 4 July 2009; accepted: 14 October 2009; published online: 19 November 2009

Introduction

Brain tumours are classified according to the type of normal tissue they most closely resemble. However, in most cases, it is not known which cell type has given rise to the tumour. Furthermore, it is unclear to what extent the type and behaviour of the tumour is determined by its cell of origin or by the genetic events that occurred in that cell.

One possible origin of CNS tumours are endogenous neural stem cells (B type) or transit amplifying cells (C type) that derive from them (Oliver and Wechsler-Reya, 2004; Sanai *et al*, 2005; Stiles and Rowitch, 2008). After the major phase of brain development is complete, a population of stem cells persists close to the walls of lateral ventricles in an extensive germinal zone known as the sub-ventricular zone (SVZ; Doetsch *et al*, 1999). These cells continue to proliferate and retain the capacity to generate neurons and glial cells. The SVZ is a complex but well-defined niche containing stem cells (type B cells), transient amplifying precursors (type C cells) and young neuroblasts (type A cells). A number of mouse models have suggested that deregulation of proliferation within the SVZ can lead to hyperplasia or tumour-like masses (Conover *et al*, 2000; Doetsch *et al*, 2002; Zhu *et al*, 2005a, b). A recent study has shown that stimulation of the PDGFRα-expressing B-type neural stem cell induces the formation of hyperplasia resembling oligodendrogliomas next to the SVZ (Jackson *et al*, 2006). However, in contrast to spontaneous tumours, this hyperplasia regresses after withdrawal of the growth factor. Activation of Ras and Akt in nestin-expressing progenitors (but not in GFAP-expressing SVZ stem cells) induces glioblastoma, a malignant astrocytoma (Holland *et al*, 2000), and nestin-expressing GFAP-negative progenitor cells deficient in INK4a/ARF and Bmi1, isolated *in vitro*, can give rise to low-grade diffuse astrocytomas (Bruggeman *et al*, 2007). GFAP-cre-mediated inactivation of Nf1 and p53 in neural progenitor and in neural stem/progenitor cells of the SVZ induces glia progenitor proliferation and ultimately malignant astrocytomas (Zhu *et al*, 2005a, b), which is accelerated by additional haploinsufficiency for PTEN (Kwon *et al*, 2008). In keeping with these observations, GFAP-cre-mediated inactivation of PTEN and p53 in progenitor cells resulted in the formation of malignant astrocytomas (Zheng *et al*, 2008). A targeted approach, in which only adult nestin-expressing cells were recombined, was used to inactivate Nf1, p53 or Nf1, p53 and PTEN, resulting in the formation of malignant gliomas (Alcantara Llaguno *et al*, 2009). In a similar approach, Wang *et al* (2009) introduced mutant p53 alongside a p53 deletion on the other allele, in addition to a deletion of Nf1 in GFAP-expressing cells, again generating glial tumours. Although these models indicate that nestin-expressing cells contained within the adult CNS can give rise to brain tumours, they do not determine whether these tumours derive from stem cells or other precursor/progenitor

cells. Most models using a GFAP-cre-mediated approach to target cells expressing GFAP during development, including neural progenitor cells and their progeny and hence do not strictly target only GFAP-expressing adult stem cells and mature astrocytes. Moreover, we do not know how different tumour suppressor genes contribute to the tumour phenotype.

We set out to investigate (i) whether the stem cell population of the SVZ can give rise to brain tumours, (ii) which tumours can arise from these cells, (iii) to what extent the phenotype of the tumour is determined by the initial combination of genetic mutations, and (iv) whether mature astrocytes can contribute to the formation of gliomas. This may ultimately answer the questions: why certain brain tumours show reproducible patterns of genetic mutations and why alterations in certain pathways are often associated with certain types of tumours.

Results

Adeno-cre and adeno GFAP-cre target stem/progenitor cells in the subventricular zone

In this study, we used mice bearing conditional alleles (flanked by LoxP sites) of Rb, p53 and PTEN, in different combinations and used an adenovirus expressing cre recombinase (either Adeno-cre or Adeno GFAP-cre) to delete these genes in stem/progenitor cells of the SVZ of adult mice.

First, we determined the distribution of cells that underwent recombination after intracerebroventricular (i.c.v.) injection of Adeno-cre into ROSA26 Lox reporter mice (R26R), which express β-galactosidase on Cre-mediated recombination (Soriano, 1999). Controls were wild-type mice injected with an adenovirus expressing green fluorescent protein (Adeno-GFP). Between 4 and 14 days after i.c.v. injection, mice were killed and their brains were analysed by histochemistry (Figure 1A and C), immunohistochemistry or immunofluorescence (Figure 1B) for β-galactosidase. Recombination and expression of β-galactosidase occurred bilaterally in a thin periventricular strip that included the ependyma and the SVZ (Figure 1A–C) up to 4–5 cell diametres deep to the ependymal surface. In Adeno-GFP injected controls, GFP expression co-localized with nestin and GFAP—markers expressed by progenitor and stem cells in the SVZ (Figure 1K–N).

As B-type of SVZ cells are considered stem cells and distinguished from other SVZ progenitor cells by their expression of GFAP (Doetsch *et al*, 1999), we also targeted these cells using an adenovirus expressing Cre (or GFP) under the control of the GFAP promoter. Adeno-GFAP–GFP injection labels a population of SVZ cells that expressed GFAP (Figure 1O–R).

Stem and progenitor cells in the SVZ can be cultured as neurospheres. To confirm that SVZ-derived progenitor cells were among cells that underwent cre-mediated recombination, we cultured neurospheres from R26R reporter mice 4 days, 1 or 2 weeks after intraventricular Adeno-cre injection. In three preparations, 8, 12, and 40% of neurospheres contained recombined cells when isolated (Figure 1D and E) but the number of spheres containing recombined cells expanded with increasing passage number, suggesting that recombined cells underwent self-renewal, a property to be expected if the recombined cells included stem cells (Figure 1E). Self-renewal of the SVZ cells was confirmed by isolation and *in vitro* propagation of the recombined cells grown as neurospheres (Jacques *et al*, 1998, 1999). In three separate experiments, 1508 cells were plated in total, of which 291 were a single cell in each well. Of these single cells, 68 (23%) self-renewed and formed a neurosphere, of which 51 (18% of all single cells) were uniformly X-gal positive. A representative example of a single cell forming an X-gal-positive neurosphere is shown in Figure 1F. Such neurospheres could be differentiated into neuronal, glial, and oligodendrocyte lineages (Figure 1G–J) and were further propagated, demonstrating their pluripotency and self-renewal capacity. This experiment further confirms that SVZ-derived progenitor cells were among cells that underwent cre-mediated recombination and that these cells can be propagated *in vitro*. In conclusion, Adeno-cre-mediated recombination targets SVZ cells that can be propagated *in vitro* and can self renew.

Inactivation of tumour suppressor genes in the stem cell compartment of the SVZ causes brain tumours

To determine which tumours could arise from these periventricular cells, we injected Adeno-cre into the ventricles of mice with homozygous floxed alleles of the key tumour suppressor genes *Rb*, *p53* (Marino *et al*, 2000) and *PTEN* (Marino *et al*, 2002), as well as the reporter gene *R26R* (Soriano, 1999) in the combinations *Rb/p53*, *Rb/p53/PTEN*, or *p53/PTEN*. We chose to target genes that are frequently altered in human brain tumours and are fundamental suppressors of neoplasia in a range of tissues (Collins, 2002). Each combination of tumour suppressors produced specific and reproducible types of tumour after a latency determined by the genotype of the mice (Figures 2 and 3, Supplementary Figure S1, Supplementary Table S1).

Rb/p53 mice developed malignant tumours after a relatively constant latency of approximately nine months (274.42 ± 27.42 days (95% CI)) (Figure 3A). An autopsy of 101 mice revealed extensive, well-demarcated forebrain tumours in 20 mice (19.8%; Figure 2A and D), typically involving lateral ventricles. They were mainly of one histological type, characterized by diffuse sheets of closely packed, undifferentiated and malignant cells (Figure 2G), which in approximately half of the tumours formed rosettes (analogous to Homer Wright rosettes (Figure 2G inset), corresponding to primitive neuroectodermal tumours (PNETs) in humans. These tumours were strongly positive for the neuronal marker, synaptophysin (Figure 2J), but negative for NeuN and neurofilament, both markers of more mature neuronal differentiation, for glial markers, GFAP (Figure 2M) and S100β, and for epithelial markers, cytokeratin and epithelial membrane antigen (EMA). The administration of Adeno-Cre into mice with additional conditional alleles of *PTEN*, (Rb/p53/PTEN mice) resulted in a considerably shorter latency before the tumours developed (100.65 ± 6.09 days (95% CI); $P < 0.001$, ANOVA with Bonferroni *post-hoc* testing; Figure 3A). An analysis of 80 mice showed the presence of a PNET in 41 animals (51.3%). The PTEN/Rb/p53 tumours had an appearance similar to Rb/p53 tumours (Figure 2B, E and H), and they showed similar mitotic rates (Figure 3B) and identical immunohistochemical properties; with positive staining for synaptophysin and negative staining for glial markers (Figure 2K and N). Furthermore, they were found in a similar location, typically

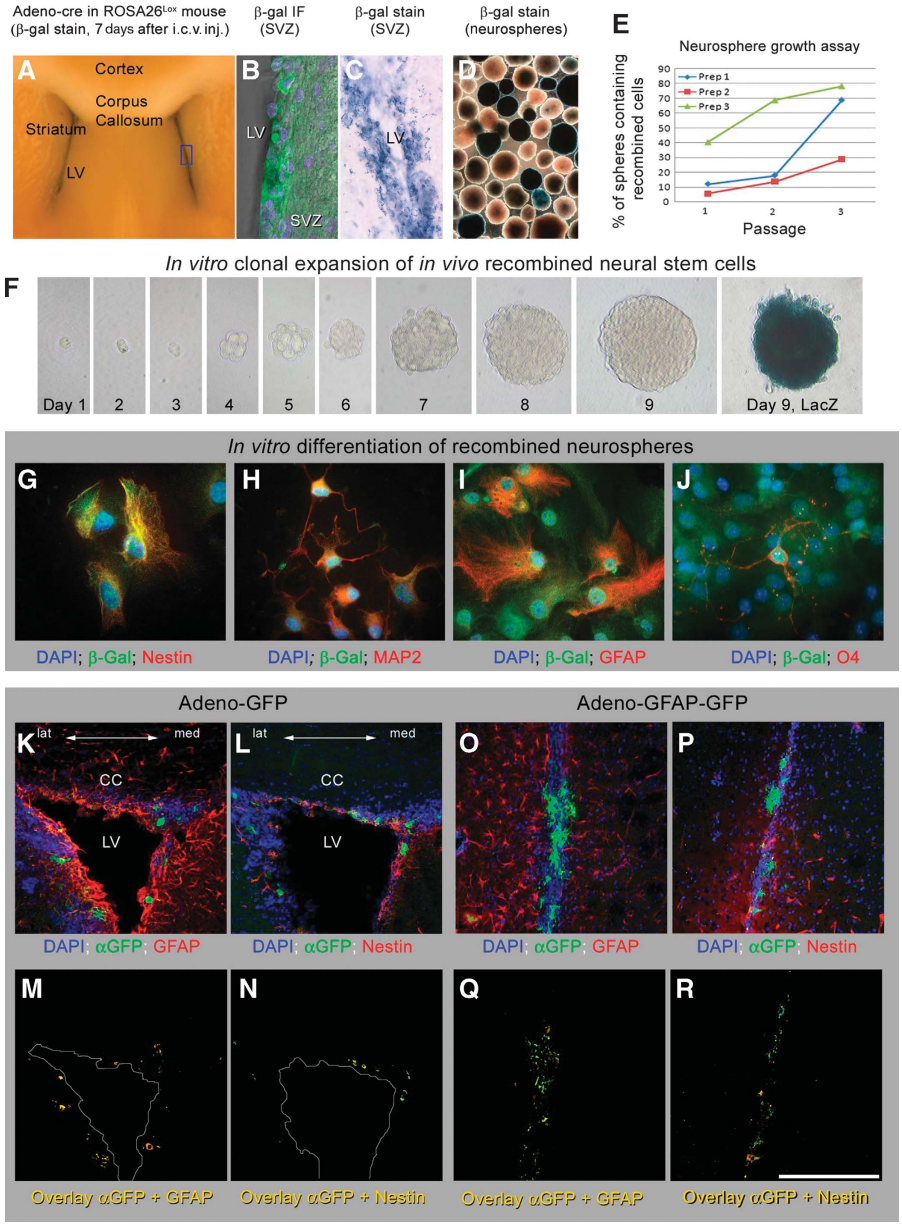

Figure 1 Intra-ventricular injections of adenovirus target a thin layer deep to the ependymal wall that includes the progenitor cells. (**A**) Coronal section through a ROSA26^{Lox} mouse 7 days after intracerebro-ventricular injection with Adeno-cre. Recombined cells are restricted to a thin periventricular region. (**B**) Superimposed confocal and phase contrast image of the lateral wall of the lateral ventricle after immunostaining against β-gal, confirming that recombination is limited to a thin layer of cells beneath the ependyma. (**C**) LacZ histochemical stain on a vibratome section shows recombination in the SVZ. (**D**, **E**) Recombined neurospheres derived from ROSA26^{Lox} mice following intraventricular injection with Adeno-cre (**D**); β-gal histochemistry on neurospheres. (**E**) Increasing proportion of positive cells during time *in vitro*. (**F**) *In vivo*-recombined, *in vitro*-expanded neural stem cells grow from single cells to neurospheres, demonstrating their ability to self-renew. Each image shows the same cell/sphere during self-renewal and growth, and on day 9 before (F9) and after LacZ staining (**F**, day 9, LacZ). (**G**–**J**) *In vitro* differentiation of *in vivo* recombined stem cells after clonal expansion from a single cell. Neurospheres were differentiated *in vitro* and double labelled for β-galactosidase (green) to detect cre-mediated recombination and a marker of differentiation (nestin, (**G**); MAP-2 (**H**); GFAP (**I**) and O4(**J**)), indicating their capability to differentiate into neuronal, glial and oligodendroglial lineages. (**K**–**N**) Confocal images of coronal sections of the lateral ventricle of wild-type mice after injection by Adenovirus–GFP: (**K**, **L**) triple-labelled images; (**M**, **N**) co-localization of GFP and nestin (**M**) or GFAP (**N**). The same cell population is targeted with Adeno-GFAP-GFP (**O**–**R**). Scale bar 200 μm (**K**–**R**).

involving lateral ventricles and extending into the forebrain. However, in contrast to the diffuse architecture of the Rb/p53 tumours, Rb/p53/PTEN tumours had a more distinctive architecture with formation of nodules and clusters of cells separated by fibrous bundles visualized by reticulin silver staining (Figure 2Q), which were also positive for the meningeal (arachnoidal) marker, EMA (Figure 2R). These data suggest that the nodular phenotype is associated with extensive invasion into the meninges. Finally, p53/Rb/PTEN tumours showed necrosis less frequently than those from Rb/p53 mice ($P = 0.001$, χ^2 test).

Targeted deletion of PTEN and p53 in SVZ cells resulted in neoplasms with an intermediate latency (225.07 ± 18.44 days (95% CI)) slightly shorter than that of Rb/p53 tumours ($P < 0.001$ ANOVA with Bonferroni *post-hoc* testing; Figure 3A) but importantly, they had an entirely different

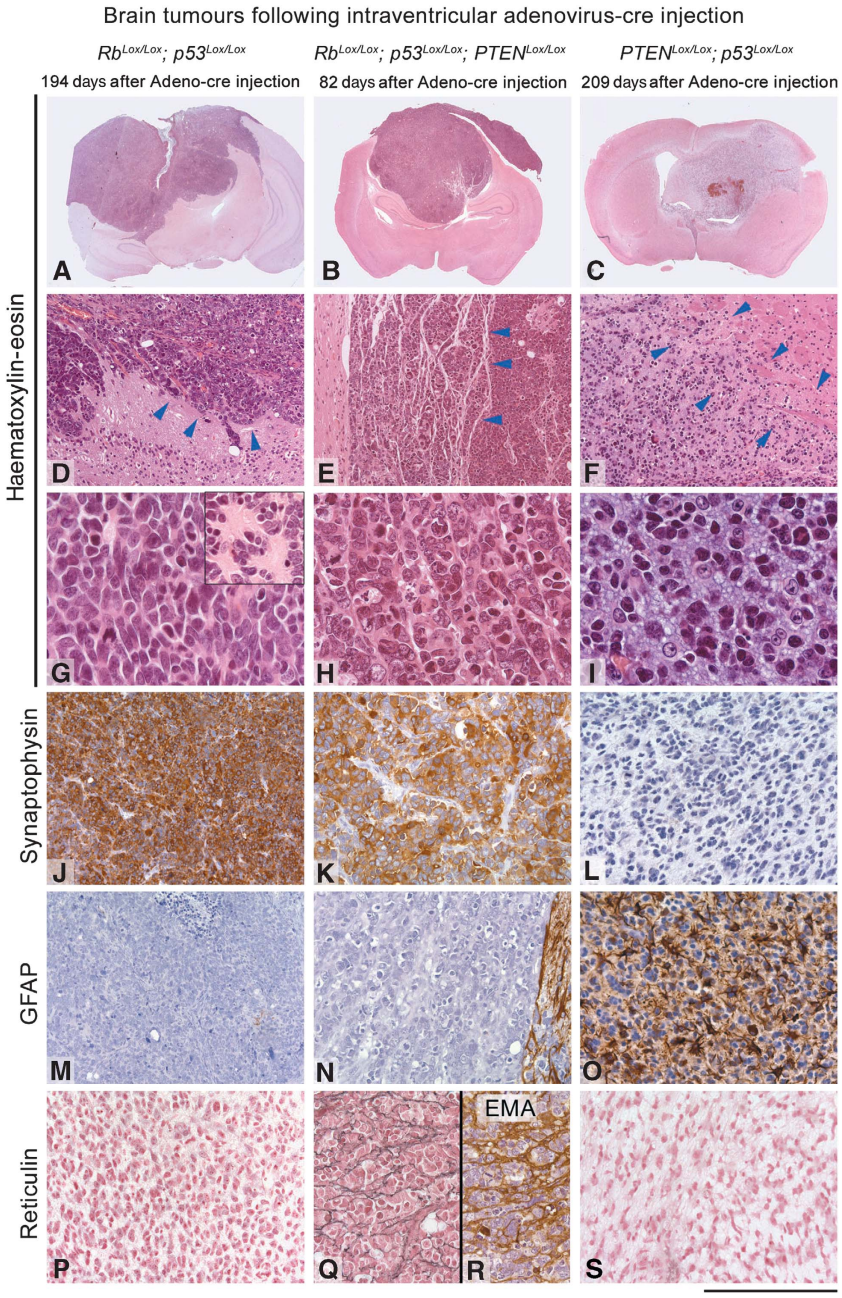

Figure 2 The phenotype of brain tumours is influenced by the initial genetic deletion: left column: tumours in Rb/p53 mice: (**A**, **D**, **G**, **J**, **M**, **P**); middle column: Rb/p53/PTEN tumour (**B**, **E**, **H**, **K**, **N**, **Q**, **R**); and right column: tumour derived from p53/PTEN mice (**C**, **F**, **I**, **L**, **O**, **S**). Panels **A**–**I** are stained with haematoxylin and eosin. (**D**) Arrowheads point to the border between tumour and the adjacent non-neoplastic brain. (**E**) Arrowheads indicate thin septae of meningeal origin that separate tumour cells into trabeculae. (**F**) The area indicated by arrowheads is the ill-defined border between tumour (left) and brain (right; 'infiltration zone'). (**G**–**I**) High-power magnification shows the morphological differences between PNET (**G**, **H**) and glioma (**I**), with rosette formation (**G**, inset) in the PNETs. (**J**–**L**) Synaptophysin immunohistochemistry shows strong positive labelling of all tumour cells in (**J**, **K**), and no expression in gliomas (**L**). (**M**–**O**) GFAP immunohistochemical labelling with no expression in PNET (**M**, **N**). The small rim on the right in (**N**) is adjacent brain that shows strong reactive gliosis, and (**O**) shows GFAP expression in all glioma cells. (**P**–**S**) The additional deletion of PTEN in a Rb/p53 background (**Q**, **R**) results in extensive desmoplastic reaction/meningeal infiltration: PTEN/Rb/p53 tumours show reticulin and epithelial membrane antigen (EMA)-positive structures separating nests of tumour cells (**Q**, **R**). No desmoplastic reaction in Rb/p53 PNET (**P**) or in PTEN/p53 gliomas (**S**). Scale bar: 5.2 mm (**A**–**C**), 440 μm (**D**–**E**), 110 μm (**G**–**I**) and 220 μm (**J**–**S**).

histological phenotype. These tumours were infiltrative and expanded from the ventricular wall laterally into the corpus callosum, striatum and cortex in a diffuse manner (Figure 2C and F). A histological analysis of 116 mice showed 28 such tumours (27%, Supplementary Table S1). They showed a biphasic pattern with cells with small dense nuclei and small amounts of eosinophilic cytoplasm, along with another population with larger, bright and vesicular nuclei and indistinct cytoplasm, set against a myxoid background (Figure 2I). Areas of micro-vascular proliferation and a type of necrosis characteristic of human high-grade gliomas ('palisading necrosis'; Louis *et al*, 2007) were also observed in some of these

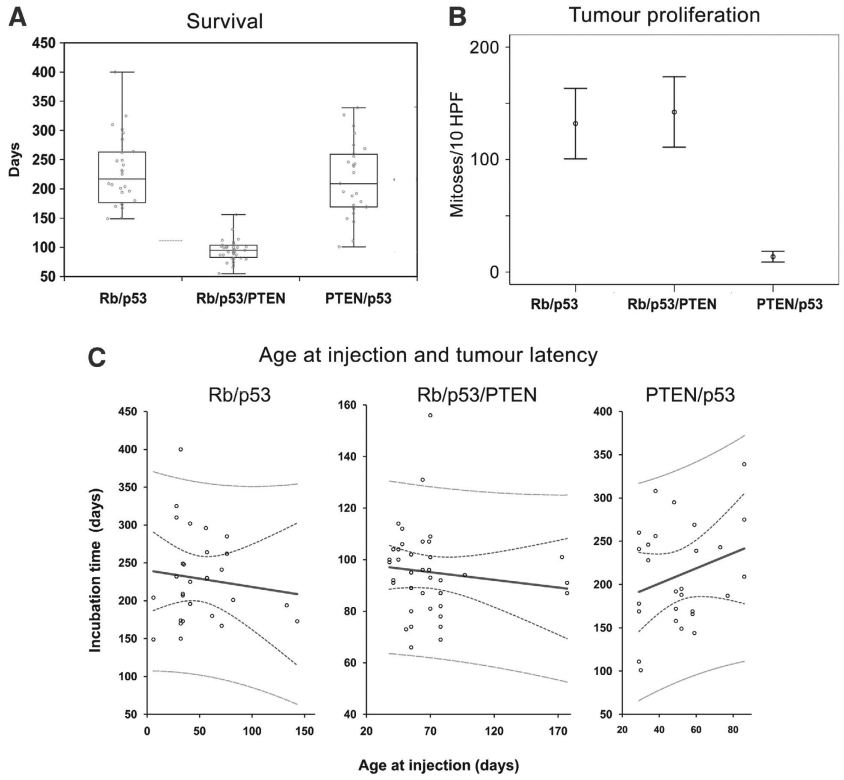

Figure 3 (**A**) The genotype determines the latency of tumour formation. Mean time (days to tumour presentation ± 95% confidence intervals). Rb/p53/PTEN has a significantly shortened latency. $P<0.05$ ANOVA, *post-hoc* Bonferroni, box plot with 95% of all samples. All tumour types were included. (**B**) The genotype determines the proliferation rate of the tumours: the graph shows mean mitotic counts per 10 high-power fields (×40 objective) ± 95% confidence intervals, PTEN/p53 differs significantly from the other genotypes ($P<0.05$ ANOVA, *post-hoc* Bonferroni). All tumours examined were gliomas in PTEN/p53mice and PNET in two other genotypes. (**C**) The tumour latency is independent of the age at injection. The graph shows the relationship between age at injection and the tumour incubation time (development of neurological signs). Polynomial regression analysis was performed. None of the genotypes showed a significant correlation between age at injection and latency. Rb/p53: $r=-0.22$, $P=0.55$; Rb/p53/PTEN: $r=-0.05$, $P=0.38$; PTEN/p53: $r=0.8$, $P=0.17$. Solid blue line, linear fit; dotted blue line, 95% confidence interval; dotted green line, 95% prediction interval. A full-colour version of this figure is available at *The EMBO Journal* Online.

tumours. The PTEN/p53 tumours had a considerably lower mitotic count (Figure 3B) compared with tumours in Rb/p53 or Rb/p53/PTEN mice ($P<0.05$, ANOVA with Bonferroni *post-hoc* testing). In contrast to Rb/p53 and Rb/p53/PTEN tumours, all p53/PTEN tumours contained a population of small neoplastic glial cells that strongly expressed GFAP (Figure 2O), but no neuronal markers (NeuN, neurofilament or synaptophysin; Figure 2L), similar to human anaplastic astrocytomas or anaplastic oligoastrocytomas, corresponding to WHO Grade III.

In addition to the tumours mentioned above, we occasionally observed other tumours, such as choroid plexus tumours ($n=13$; 12.8%; mean latency of 370.6 ± 20.4 days (95% CI); Supplementary Figure S1) in Rb/p53 mice that survived beyond the time at which most PNET-like tumours would have formed. Other tumours included osteogenic skull tumours in PTEN/p53 mice ($n=21$; 18.1%; Supplementary Figure S1) and meningiomas (predominantly in Rb/P53/PTEN mice; $n=20$; 25%). In one instance, there was a diffuse infiltrative tumour resembling high-grade glioma together with the more 'typical' PNETs that are commonly found in those mice (in two Rb/p53/PTEN mice; Supplementary Figure S2, Supplementary Table S1). As the number of actively proliferating SVZ stem cells gradually decreases during lifetime (Alvarez-Buylla and Temple, 1998), the age at injection may influence the type and number of targeted cells. We therefore analysed whether the age at injection correlates with the latency of tumour development. Using polynomial regression analysis, we found that none of the genotypes showed a significant correlation between age at injection and latency of tumour development (Figure 3C).

Microneoplasia arises from recombined SVZ cells and precedes brain tumours

To determine where the tumours arose from, we killed Rb/p53, Rb/p53/PTEN and PTEN/p53 mice after intra-ventricular delivery of Adeno-cre or Adeno-GFP before expected tumour formation. We noted small collections of cells with atypical nuclear features, perivascular collections of atypical cells or well-formed nodules of tumour cells at the dorsolateral angles of the lateral ventricles. These areas contain large collections of stem and progenitor cells in the adult brain (Figure 4). Instead, such lesions were observed in the medial wall only in one instance. All lesions arose as a result of cre-mediated recombination, as they expressed the recombination marker β-galactosidase (Figure 5D and G). In contrast, we did not observe β-galactosidase expression or SVZ microneoplasia when Adeno-cre was injected in different areas, such as striatum or hippocampus (Figure 6J–M). Although nestin- and GFAP-positive stem/progenitor cells may also exist in the medial wall (Figure 1K–R; Alvarez-Buylla *et al*,

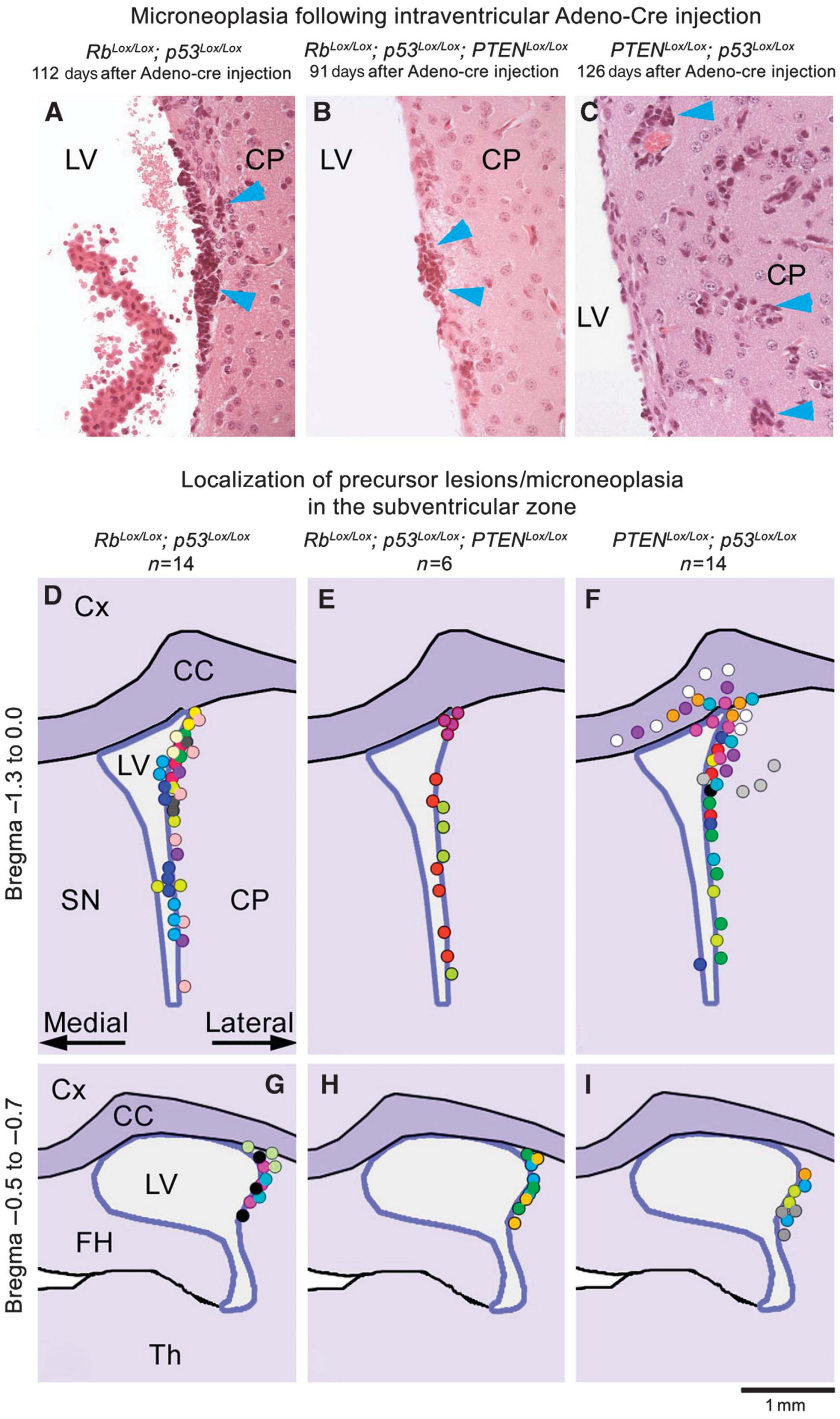

Figure 4 Small neoplastic lesions ('microneoplasia') after intraventricular Adeno-cre injection precede brain tumours. Upper row (**A**–**C**): Histological appearance of small neoplastic lesions located beneath the ependymal layer of the lateral wall of the ventricle. Occasionally, perivascular spread was seen in PTEN/p53 mice (**C**). (**D**–**I**) Schematic representation of precursor lesions: cumulative maps showing the localization of small lesions. Each dot represents microneoplasia or a focal cluster of tumour cells (approximately 200 μm). Each colour represents an individual animal. The map summarizes lesions in 14 Rb/p53 mice, 6 Rb/p53/PTEN mice and 14 PTEN/p53 mice. The upper schematic panel (**D**–**F**) summarizes lesions in the anterior ventricular region (Bregma −1.3 to 0.0) and the lower panel (**G**–**I**) represents the posterior region (Bregma −0.5 to −0.7). The microneoplastic lesions are almost exclusively localized beneath the lateral wall of the ventricles and in the lateral corner of the ventricle, and may occasionally protrude to the opposite wall. Although Rb/p53 and Rb/p53/PTEN lesions tend to remain locally clustered, PTEN/p53 lesions often spread laterally and into the corpus callosum, in keeping with the more infiltrative nature of these tumours (**F**). One small lesion in an Rb/p53 animal (**D**, yellow dot) was observed extending to the medial side but may not have arisen there and one small lesion in a PTEN/p53 animal arose from the medial surface (**F**, blue dot), indicating a very strong preference for the lateral/dorsolateral walls, consistent with the presumed localization of SVZ stem cells. Cx, cortex; CC, corpus callosum; LV, lateral ventricle; SN, septal nuclei; FH, fimbria hippocampi and Th, thalamus.

2008), the more predominant presence of precursor lesions in the lateral wall suggests that permissive stem/progenitor cells may be more abundant in the lateral wall and that the predominance of lesions in the later wall reflect the stochastic events of cre-mediated recombination. To demonstrate that tumours originated from cells that underwent Adeno-cre mediated recombination, and to address the issue that cre-mediated recombination may not be equally effective at different lox sites (Soriano, 1999; Loonstra *et al*, 2001; Vooijs *et al*, 2001), we microdissected a series of tumours derived from mice of all genotypes and verified recombination by PCR (Marino *et al*, 2000). All tumours showed recombination suggesting that these tumours arose independently from complete recombination of stem or progenitor cells (Figure 5A–C) and that cre-mediated recombination was consistent and complete. To further identify recombined precursor lesion and tumour cells, their relationship to the SVZ and the infiltration pattern into non-recombined surrounding CNS parenchyma, we stained for the recombination marker β-galactosidase as surrogate marker for the genes $p53^{lox}$, Rb^{lox} and $PTEN^{lox}$, and observed that it was expressed in all precursor lesions and tumours (Figure 5D–I). In keeping with the localization of adenovirus-mediated recombination (Figure 1A–C), the SVZ also showed β-galactosidase labelling along the lateral, dorsal and medial walls, but only one instance of precursor lesions in the medial wall (Figure 4F). This suggests that tumours arise from specific populations, that is, the neurogenic portion of the lateral SVZ, and it is unlikely that other cell populations, such as ependymal cells, contribute to tumour formation.

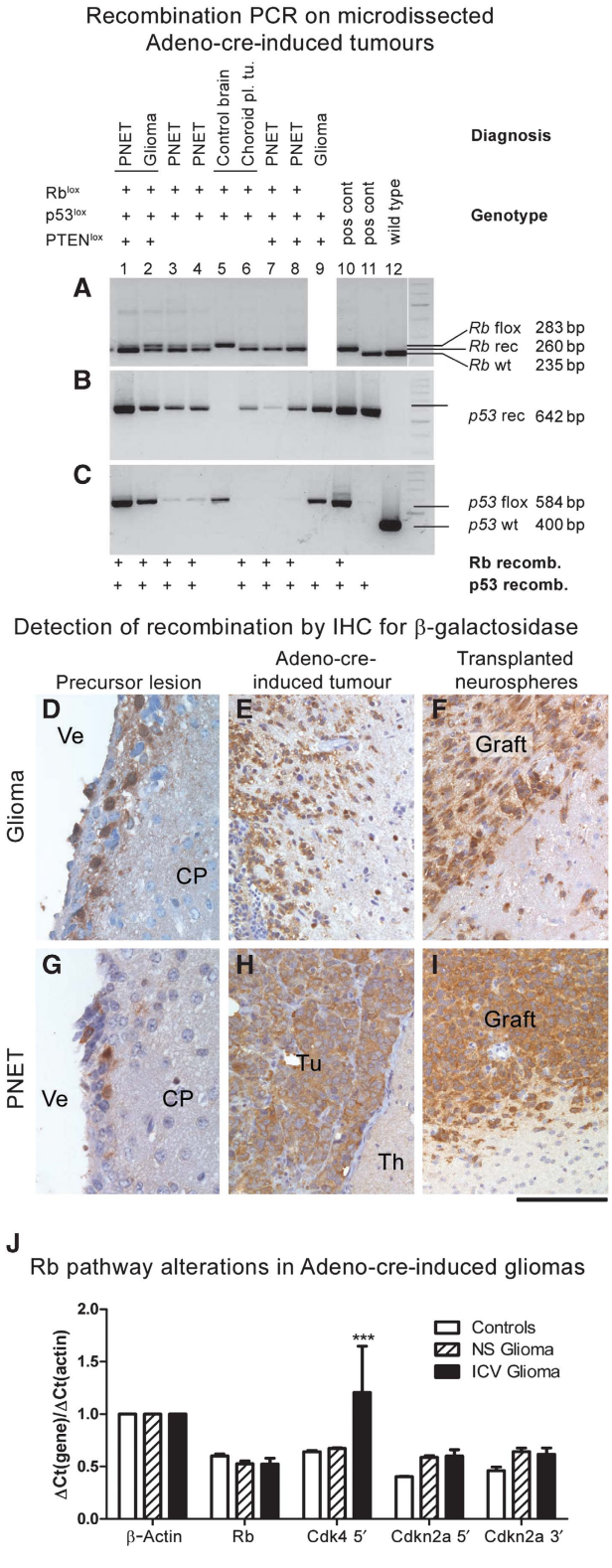

GFAP-expressing B-type SVZ stem cells are the origin of intrinsic brain tumours

We then explored whether the tumours were derived from SVZ type B cells, which are GFAP-expressing stem cells. To this end, we performed injections using an adenovirus expressing Cre (or GFP) under the control of the GFAP promoter (Figure 1O–R, Supplementary Figures S1 and S2). Injection of Adeno-GFAP-Cre into the ventricles of Rb/p53, Rb/p53/PTEN or PTEN/p53 mice resulted in the formation of tumours, histologically identical to those observed after injections of Adeno-Cre (Supplementary Figure S2). These data support the hypothesis that GFAP-expressing cells in the SVZ (B-type SVZ cells) can give rise to either PNET or glioma depending on the combination of genes that are disrupted.

Figure 5 Gene recombination in experimentally induced brain tumours: (**A–C**) recombination PCR on microdissected tumours demonstrates recombination of floxed genes in brain tumours: Lanes 1 and 2: rare instance of two histologically distinct tumour phenotypes in the same brain (mouse genotype Rb/p53), both showing recombination of Rb (**A**) and p53 (**B**, **C**). Lanes 3, 4, 7 and 8 are further examples of recombination in PNETs, whereas lane 6 shows recombination in other tumour types and no recombination is seen in control tissue. Lane 8 shows glioma with recombination of p53. PTEN recombination was not tested in these tumours. (**D–I**): Immunohistochemical detection of β-galactosidase in recombined cells of precursor lesions (**D**, **G**), Adeno-cre-induced primary brain tumours (**E**, **H**) and in tumours derived from grafted neurospheres that were recombined *in vitro* before implantation (**F**, **I**). As all mice carried the ROSA26lox gene, recombination results in β-galactosidase expression in recombined SVZ cells, microneoplasia and tumours but not in uninfected brain parenchyma. Ve, ventricle; CP, caudoputamen; Tu, tumour, Th, thalamus. Scale bar: 60 μm (**D**, **G**); 120 μm (**E**, **F**, **H**, **I**). (**J**) Expression analysis of the Rb pathway in primary tumours (solid bars) and grafts (shaded bars). RNA extracted from two normal forebrains served as controls (white bars). Gene transcripts: Rb, Cdk4, Cdkn2a 5′ (p16/Ink4a and p19/Arf), Cdkn2a 3′ (p19/Arf) and β-actin. The 5′ transcript of Cdk4 is significantly ($P<0.001$) upregulated in brain tumours, whereas there is a statistically non-significant upregulation of p16/Ink4a and p19/Arf transcripts.

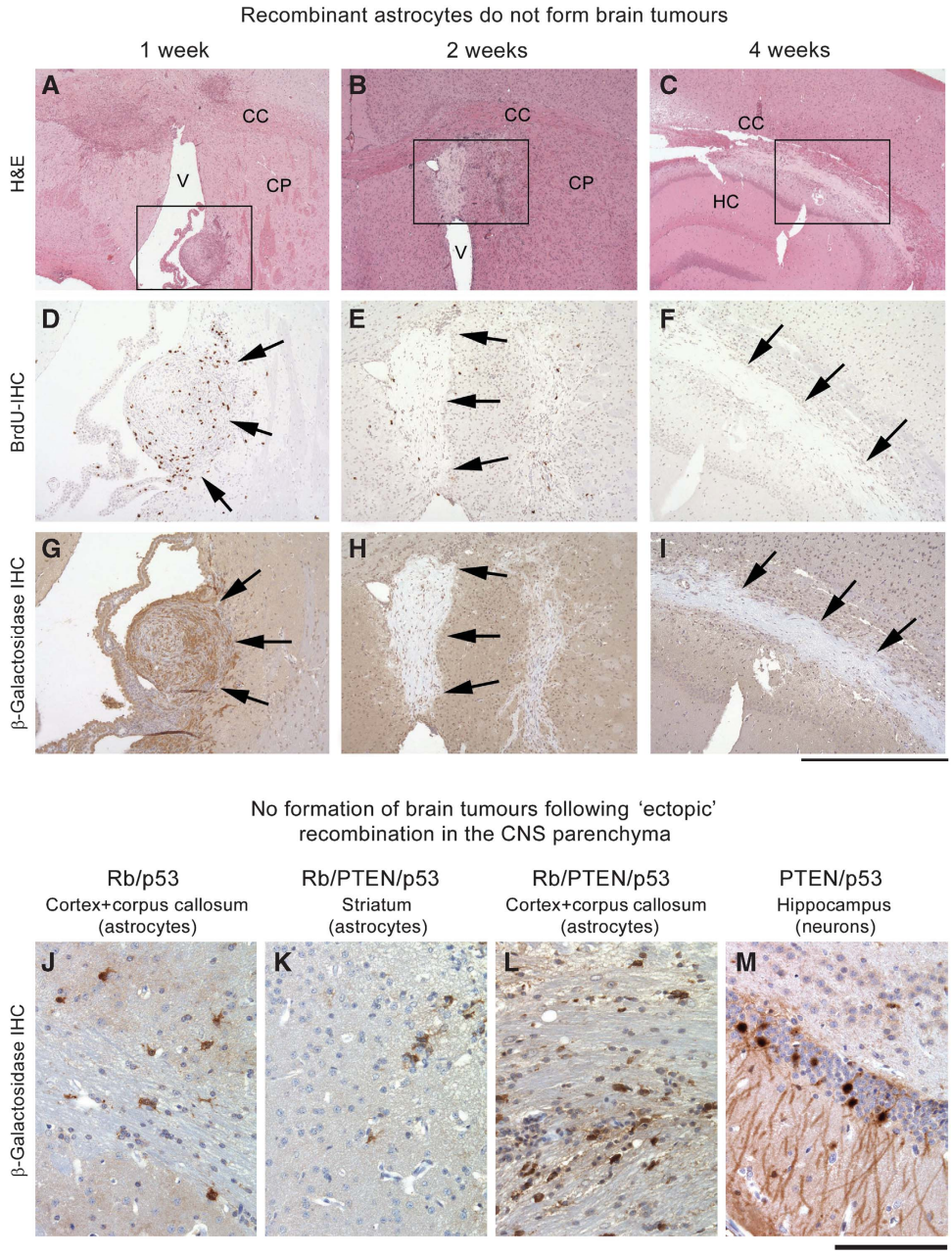

Figure 6 Recombinant astrocytes do not form brain tumours. *In vitro* recombined astrocytes (PTEN/Rb/p53) were implanted into the striatum of recipient mice from identical genetic background. At 1 week after grafting (**A**, **D**, **G**) there are several nodules of spindle shaped cells in several locations, such as the ventricle, attached to the striatum (boxed area), immunostaining for BrdU shows frequent proliferating cells. (**G**) Recombined cells show expression of β-galactosidase (arrows) in the graft, but only background staining of the neuropil. After 2 weeks, the grafts have largely degenerated into gliotic scar tissue and show only infrequent proliferating residual cells (**E**, BrdU IHC). (**H**) β-galactosidase IHC shows absence of staining in these degenerate grafts, notably, this tissue gives less background stain than CNS tissue. At 4 weeks (**C**, **F**, **I**) only scar tissue remains and no more proliferating cells are seen (**F**), and β-galactosidase immunoreactivity is absent. Scale bar: 1.3 mm (**A**–**C**), 550 μm (**D**–**I**). (**J**–**M**) Ectopic injection of Adeno-cre recombines grey and white matter astrocytes but does not cause their neoplastic transformation *in vivo*. Occasionally, hippocampal neurons were recombined, but no tumours formed.

The latency of Adeno-cre- and Adeno-GFAP-cre-induced gliomas in PTEN/p53 mice did not show a statistically significant difference (mean 210.6 versus 234.2, $P = 0.42$).

In vitro recombined stem cells form tumours identical to those induced by intraventricular Adeno-cre

To confirm that tumours were derived from SVZ neural stem cells or their immediate progeny, we derived neurosphere cultures from the compound loxP mutant mice described above and induced recombination after 20–30 days *in vitro* by adding Adeno-cre to the cultures. This resulted in recombination in 70–90% of the neurospheres and a faster growth rate of the recombined spheres. After 2–4 passages in culture, these neurospheres were implanted into the striatum of non-recombined mice of similar genetic background (Supplementary Table S2). In 32 of 78 mice (42%), these grafts led to the development of malignant tumours. Transplanted Rb/p53 spheres ($n = 8$ of 32 mice (25%)) and

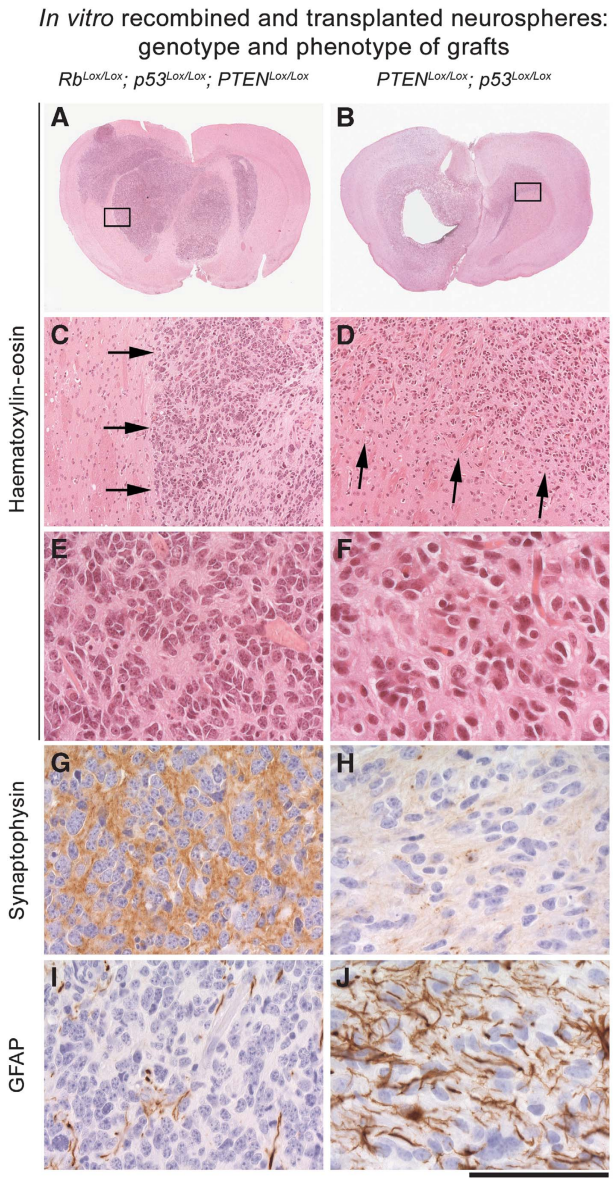

Figure 7 *In vitro*-recombined neurospheres generate tumours with a phenotype that resembles those generated by *in vivo* recombination. Left column (**A**, **C**, **E**, **G**, **I**): tumours derived from injection of Rb/p53/PTEN neurospheres. Right column (**B**, **D**, **F**, **H**, **J**): tumours derived from injection of p53/PTEN neurospheres. Panels (**A**–**F**) haematoxylin and eosin. Arrows in (**C**) and (**D**) show a well-demarcated (**C**) border in PNET or a diffuse infiltration into the CNS (**D**). Panels (**G**, **H**): synaptophysin is expressed in PNET (**G**) but not in gliomas (**H**). Panels (**I**, **J**) GFAP is not expressed in PNET (**I**) but clearly identifiable in neoplastic astrocytes in gliomas (**J**). Scale bar: 4 mm (**A**, **B**), 350 μm (**C**, **D**) and 90 μm (**E**–**J**).

Rb/p53/PTEN spheres ($n=13$ of 24 mice (54%)) developed tumours (Figure 7A, C and E; Supplementary Table S2) similar to the PNET seen after *in vivo* recombination. Furthermore, these grafts expressed synaptophysin but were predominantly negative for GFAP (Figure 7G and I). In contrast, p53/PTEN spheres mostly formed infiltrative glial tumours, which expressed GFAP but not synaptophysin ($n=8$ of 22 mice, (36%)) (Figure 7B, D, F, G and J; for experimental details see Supplementary Table S2). Therefore, *in vitro* recombination of neurospheres reproduced the phenotype of tumour formed after *in vivo* recombination. These results further support the hypothesis that these brain tumours are derived from stem/progenitor cells of the SVZ (Rietze and Reynolds, 2006).

PTEN–p53-deficient gliomas show alterations of the Rb pathway

Human gliomas frequently show disruption of the p53 pathway through loss of ARF, or less frequently through amplification of MDM2 and a disruption of the RB pathway through loss of INK4A and CDK4 upregulation (for review, see Holland (2001)). To test whether the *Rb* pathway was also altered in the gliomas in our model system, induced by inactivation of PTEN and p53, we analysed transcriptional activity of the Rb pathway in three primary (intraventricular Adeno-cre induced) tumours as well as in three tumour grafts derived from transplanted *in vitro* recombined stem cells. The RNA extracted from two normal forebrains served as controls. We assayed the Rb pathway gene transcripts Cdk4, Cdkn2a (p16/Ink4a and p19/Arf), Rb and β-actin as control. The 5′ transcript of Cdk4 was significantly ($P<0.001$) upregulated in brain tumours, indicating increased CDK4 activity. The Cdkn2a 5′ probe detects both p16/Ink4a and p19/Arf transcripts, whereas the Cdkn2a 3′ probe only detects p19/Arf. The levels of both transcripts were similar, suggesting both transcripts represent p19/Arf rather than p16/Ink4a. The values indicate a mild upregulation of p16/Ink4a and p19/Arf transcripts, which does not reach statistical significance. Increased p19/Arf transcription is likely to be a result of a positive feedback loop in response to absent p53 protein (Tao and Levine, 1999; Sherr and Weber, 2000). Interestingly, there was no upregulation in grafts derived from transplanted neurospheres.

Brain tumours are not derived from astrocytes lacking Rb, p53 and PTEN

To determine, whether other GFAP-expressing cells of the adult CNS, most importantly astrocytes, can contribute to the formation of tumours, we derived astrocytes from the forebrains of P2-4 Rb/p53/PTEN, Rb/p53 or PTEN/p53 mice, and tumour suppressor genes were recombined by adding Adeno-cre *in vitro*. The cre-mediated recombination caused a significant increase in proliferation and loss of differentiation. The cells were collected after 2–5 passages and engrafted into the striatum of adult recipient mice of a similar genetic background. Transplantation of at least 10^5 recombined cells of various genotypes (see Supplementary Table S3) into 35 mice did not result in a single viable tumour after incubation times up to 413 days. To follow the *in vivo* growth of these astrocytes more closely, and to exclude technical factors, we set up short-term experiments and grafted $0.5–1\times10^6$ cells per animal. The viable cells were detectable up to two weeks post transplantation but then degenerated leaving gliotic scars at 4–6 weeks after grafting (Figure 6A–J). It is unlikely that this was due to graft rejection, as both the graft and the host genetic background matched very closely and no significant inflammatory response was seen. However, to exclude this possibility, astrocytes lacking Rb/p53/PTEN were grafted into the caudoputamen of 11 nude mice that which were killed at 2 and 4 weeks after grafting and Rb/p53-deficient astrocytes were grafted into 10 nude mice that were analysed 2, 4 and 14 weeks after transplantation. No viable cells could be detected

in these mice beyond the 4-week time point. Finally, we adapted the astrocyte culture conditions more closely to those of neurospheres. After eight passages, astrocytes were propagated for additional 4 passages as free-floating 'astrospheres' and then grafted into five mice of a matched genotype. Again, no tumour formed after up to 134 days of incubation (Supplementary Table S3).

We further wanted to exclude that astrocytes instead of, or in addition to, SVZ stem cells have a pathogenetic role in the formation of brain tumours; mice with intended SVZ injections that missed the target and did not result in a LacZ-positive SVZ were analysed for the presence of recombined cells in 'ectopic' areas, such as cortex, striatum, hippocampus and thalamus, (Figure 6J–M and Supplementary Table S4). A total of 12 Rb/p53 mice, 7 Rb/p53/PTEN mice and 5 PTEN/p53 mice were injected and killed after time points when SVZ-derived tumours should have occurred. Recombination in grey and white matter astrocytes and occasionally in mature neurones of the hippocampus was detected by immunohistochemical labelling of β-galactosidase (Figure 6J–M). None of the mice with proven ectopic injections (i.e. no labelling of the SVZ) had developed a tumour, confirming that mature astrocytes and other cells of neural lineage outside the SVZ do not contribute to brain tumour formation.

Cre toxicity is not relevant for the tumour phenotype

As cre may exert toxicity *in vitro* (Loonstra *et al*, 2001) and *in vivo* (Forni *et al*, 2006; Naiche and Papaioannou, 2007) by inducing apoptosis as well as genomic instability, we ruled out a direct, cre-mediated effect on cells in control experiments *in vitro* and *in vivo*. Several *in vitro* experiments were conducted with $ROSA26^{lox}$ cell cultures as control. In addition, a series of experiments consisted of Adeno-GFP controls. No accelerated growth suggestive of neoplastic transformation was seen in cre-treated cultures.

Excessive levels of cre expression may transiently occur after intraventricular injection of Adeno-cre or Adeno-GFAP cre. These cells are likely to be negatively selected (Forni *et al*, 2006; Naiche and Papaioannou, 2007), but in contrast to transgenic expression of cre recombinase under the control of a permanently active promoter, adenovirus-mediated expression of cre recombinase decreases, and leaves progeny of cre-infected cells with minimal or no cre at all. Further, cre may cause genomic instability, an effect that is likely to increase mutation rates, but injected virus titre was kept constant across experiments and as Cre expression is expected to be similar across all genotypes and would also to have occurred in heterozygous controls that never developed tumours, cre is unlikely to have an overall effect on the phenotype. A further control consisted of astrocytes derived from mice carrying the $Rb^{lox/lox}$ or the $p53^{lox/lox}$ alleles alone. We also infected control cultures with Adeno-GFP. No noticeable difference of apoptotic rate was seen between different genotypes and between different viruses.

Discussion

Our study shows that stem/progenitor cells in the lateral wall of the SVZ in the adult brain are the origin of intrinsic brain tumours. Stem/progenitor cells form brain tumours in a cell-autonomous manner, whereas astrocytes are not capable of malignant transformation and brain tumour formation, independent of their location. We also found that the combination of growth and differentiation signals, that is, activated oncogenic pathways, is a major determinant of the brain tumour phenotype.

Adult stem/progenitor cells of the lateral SVZ wall are the origin of brain tumours

We show here that the stem cell compartment of the SVZ is a source of brain tumours of diverse histological phenotypes, either of glial or of primitive neuroectodermal lineage. Deletion of *p53* and *Rb* in the SVZ leads to PNETs with evidence of neuronal differentiation, similar to the human counterparts. Additional loss of PTEN does not alter the differentiation of tumours but is associated with a change in the architecture of the tumour, possibly associated with meningeal invasion (Figure 2Q and R). In contrast, loss of p53 and PTEN in the SVZ stem cell compartment results in a glioma phenotype with GFAP-positive tumour cells and a morphology resembling anaplastic oligoastrocytomas.

The occurrence of 'microneoplasia' in the lateral wall of the SVZ shows that cells in this location can be the origin of intrinsic brain tumours and is in keeping with other reports in which small lesions precede the development of tumours, either in the form of proliferating astrocytes (Zhu *et al*, 2005a, b), or of progenitor cell expansions in the subventricular zone (Xiao *et al*, 2002; Alcantara Llaguno *et al*, 2009). Mouse models for medulloblastoma histogenesis showed a progression from focal hyperplasia/preneoplasia of the external granular layer to medulloblastoma (Marino *et al*, 2000; Yang *et al*, 2008; Kessler *et al*, 2009).

Several genetic mouse models have been generated to address the histogenesis of intrinsic brain tumours. Activating oncogenic pathways in GFAP- or nestin-expressing cells in the forebrain results in the formation of gliomas, but no primitive neuroectodermal tumours have yet been described. Activation of Ras and Akt in nestin-expressing stem/progenitor cells induces glioblastoma (Holland *et al*, 2000), and nestin-expressing GFAP-negative progenitor cells deficient in INK4a/ARF and Bmi1, isolated *in vitro*, can give rise to low-grade diffuse astrocytomas (Bruggeman *et al*, 2007). Inactivation of the Rb protein family (Rb, p107 and p130) in parenchymal astrocytes and GFAP-expressing stem cells results in diffuse tumours in the entire CNS and in expanded SVZ regions, but this model does not analyze whether these diffuse neoplasms were derived from transformed mature astrocytes or from stem/progenitor cells during postnatal development (Xiao *et al*, 2002). In this model, additional deletion of PTEN, but not of p53, accelerates glioma formation but does not show histological signs of tumour progression. In a modified approach (Xiao *et al*, 2005), the same transgenic mouse strain was used in which Rb, p107, p130 and also PTEN were inactivated in cortical astrocytes. This resulted in focal neoplastic lesions; however, contribution, for example, of subcallosal stem cells to tumourigenesis remains a possibility. The GFAP-cre-mediated inactivation of NF1 or NF1/p53 in neural stem/progenitor cells of the SVZ induces glia progenitor proliferation and ultimately malignant astrocytomas (Zhu *et al*, 2005a, b), which can be accelerated by haploinsufficiency for PTEN (Kwon *et al*, 2008). Again, the question remains whether these neoplasms are solely derived from the GFAP-expressing

stem/progenitor population in the SVZ of potentially from neural precursor populations during CNS development or even from adult astrocytes. In keeping with this, GFAP-cre-mediated inactivation of PTEN and p53 in neural progenitor cells causes malignant astrocytomas (Zheng *et al*, 2008). Finally, in a more cell-selective approach, malignant gliomas were generated by inactivation of the tumour suppressor genes Nf1/p53 or Nf1/p53/PTEN in adult, nestin-expressing stem/progenitor cells (Alcantara Llaguno *et al*, 2009). However, although this model bypasses developmental recombination, targeting of stem and progenitor cells remains a possibility.

The combination of genotypes determines the brain tumour phenotype

Our model system suggests that the combination of initial genetic mutations strongly influences the phenotype of brain tumours. Although previous studies have successfully generated either gliomas or PNET/medulloblastomas, we show here that the same stem/progenitor cell is capable of formation of both types, depending on the initiating signal. Inactivation of Rb and p53 causes primitive neuroectodermal tumours whereas PTEN and p53 deletion in SVZ stem cells results in gliomas. It can be hypothesized that a 'progenitor compartment' may contain subgroups of functionally different cells that are differentially susceptible to a given combination of oncogenic signals. Medulloblastomas arising in GFAP-cre; $Rb^{Lox/Lox}/p53^{Lox/Lox}$ compound mutant mice (Marino *et al*, 2000) are histologically indistinguishable from the supratentorial PNET seen in our model, despite arising from distinct stem/precursor populations. The histological similarity of tumours arising from distinct precursors further supports the hypothesis that stem/progenitor cell (de-) differentiation depends on individual signals, in this case introduced by activation of specific oncogenic pathways. In keeping, previous studies show that GFAP-cre-mediated inactivation of PTEN and p53 in neural progenitor cells causes malignant astrocytomas (Zheng *et al*, 2008), similar to those arising from the SVZ in our model.

The diversity of tumour phenotypes in the mouse models described above raises important questions regarding the relationship between stem cell differentiation and the oncogenic growth signal, and offers several hypotheses: (i) different populations of stem/progenitor cells are committed to neuronal or glial differentiation and specific oncogenic growth signals further drive them either to primitive neuronal (PNET) or glial (glioma) tumour growth. In our model, all SVZ stem/progenitor cells would be initially targeted, but initial PTEN/p53 mutations would only give the glial progenitor an advantage over other progenitors, resulting in glioma formation. Initial deletion of Rb will instead advance neuronal precursors to form a PNET, even in the presence of concomitant PTEN and p53 deletion. (ii) A single 'tumour progenitor' cell type in the SVZ produces a tumour with either glial or primitive neuronal differentiation depending on the tumour-initiating genetic alterations, or (iii) different types of glial or neuronal committed progenitors generate distinct tumours independent of the genetic alteration. We consider the first scenario as the most likely, followed by the second hypothesis, both of which are in keeping with previous observations and hypotheses, that there are 'progenitor compartments', competent to produce tumours. In keeping with this model, a stem/progenitor cell with Rb and p53 mutations could change into a neuroblast phenotype (type A cells), giving rise to the neural phenotype of a PNET. Instead the PTEN and p53 mutations may target a subpopulation that would give rise to oligodendrocytes and hence develop a glial phenotype with variable oligodendroglial features. Furthermore, our data indicate that an initial mutation of Rb has an important role in determining the PNET phenotype, a mechanism previously unknown, but does not preclude the role of this pathway in glioma progression in our model; gliomas induced by intraventricular cre in PTEN/p53 mice showed upregulation of CDK4, a kinase that phosphorylates and inactivates Rb and thus activates the cell cycle. However, in contrast to other models that show loss of p16 in gliomas induced by p53 mutation and deletion and co-deletion of NF1 in GFAP-expressing precursor cells (Wang *et al*, 2009), we found a slight upregulation of Cdkn2a 5′ (p16/Ink4a and p19/Arf) as well as of Cdkn2a 3′ (p19/Arf alone), probably representing p19/Arf rather than p16/Ink4a. This is best explained by the primary deletion of p53 in our gliomas, resulting in p19ARF upregulation to inhibit Mdm2, in an attempt to stabilize and activate p53 (Tao and Levine, 1999; Sherr and Weber, 2000). The involvement of the Rb pathway at a later stage in our glioma model underlines the importance of the sequence of mutations in determining the tumour phenotype.

Astrocytes are not capable of brain tumour formation

Several reports indicate that transformed astrocytes can form brain tumours (Holland *et al*, 1998; Ding *et al*, 2001; Sonoda *et al*, 2001; Bachoo *et al*, 2002; Blouw *et al*, 2003; Uhrbom *et al*, 2005; Xiao *et al*, 2005). Contrary to our paradigm, these models used different approaches to generate tumours from astrocytes: (i) Expression of oncogene or an activated signal-generating protein alone in astrocytes, such as ras-Akt or p21-ras (Ding *et al*, 2001; Sonoda *et al*, 2001), (ii) deficiency for the tumour suppressor ink4a/Arf alongside with the overexpression of an oncogenic signal such as k-ras (Holland *et al*, 2000; Uhrbom *et al*, 2005), Cdk-4 (Holland *et al*, 1998), or EGFR-vIII (Bachoo *et al*, 2002), (iii) expression of SV40 or of V12ras in an HIF-1α null background- (Blouw *et al*, 2003) or (iv) by expressing h-ras and Akt in GFAP-expressing stem/progenitor cells, either combined in a wild-type or in a $p53^{+/-}$ background (Marumoto *et al*, 2009). However, the relevance of these studies for the formation of malignant gliomas from *in vitro*-transformed astrocytes has recently been challenged: first, *in vitro* and *in vivo* cellular targeting selects for a less mature (hence more stem-like) astrocyte lineage, and second, transformation-competent astrocytes can only be cultured from neonatal brains, adding a possible multipotent cell to the transformed population (Stiles and Rowitch, 2008).

In contrast to the above reports, we present evidence from two complementary experimental approaches that mature peripheral astrocytes are not capable of generating brain tumours: firstly, astrocytes derived from post-natal brains, recombined *in vitro* proliferate strongly *in vitro* but consistently fail to generate tumours *in vivo* (Figure 6A–I), in contrast to mutated and transplanted stem cells that do form malignant brain tumours (Figure 7). Second, recombination of astrocytes in adult brains outside of known neurogenic regions, (i.e. cortex, striatum, thalamus; Figure 6J–M) also does not generate tumours. We conclude that activation

of the same pathways that readily generate intrinsic brain tumours from SVZ stem/progenitor cell is not capable of tumour formation from parenchymal or ectopically transplanted astrocytes.

Neural stem/progenitor cells form brain tumours in a cell-autonomous manner

It has been debated whether formation of brain tumours is a cell-autonomous event, and how critical the local environment (i.e. SVZ versus non-neurogenic regions) is for the formation of tumours (seed and soil hypothesis; for review, see Fidler (2003)). We show here that both tumour formation and tumour phenotype are cell autonomous. Neural stem/precursor cells generate brain tumours, independent of their location; inactivation of tumour suppressor genes in SVZ stem/progenitor cell gives rise to tumours of a specific phenotype depending on the combination of mutations. Stem cells derived from the neurogenic SVZ can be recombined *in vitro* and form brain tumours of the same phenotype as their *in vivo*-induced counterparts, despite being 'ectopically' transplanted into a non-neurogenic region within the CNS. Conversely, astrocytes with identical mutations are non-tumourigenic, independently of their location—parenchymal or ectopically grafted.

As SVZ stem/progenitor cells also exist in humans and contribute to neurogenesis, it is likely that somatic mutations in the SVZ stem cell compartment cause brain tumours. There are obvious differences between the spectrum of mutations in human brain tumours and the genes that are targeted to generate mouse models of brain tumours. They can be explained by diverse initiating mutations that may have affected a different (up-or downstream) molecule of the same pathway. Furthermore, the importance of initial Rb pathway mutation in the pathogenesis of PNETs in our model (the Rb pathway has hardly been investigated in human PNET) may be explained by different population of tumour-initiating cells. In keeping with the involvement of the Rb pathway in human gliomas, we found that gliomas induced by PTEN/p53 mutations show an involvement of the Rb pathway ($p19^{ARF}$, corresponding to $p14^{ARF}$ in humans) later during their progression (Figure 5J).

Materials and methods

Transgenic mice

The following genotypes were used: $R26R^{LoxP/LoxP}$; $Rb^{LoxP/LoxP}$; $p53^{LoxP/LoxP}$ (short: Rb/p53) or $R26R^{LoxP/LoxP}$; $PTEN^{LoxP/LoxP}$; $p53^{LoxP/LoxP}$; $Rb^{LoxP/LoxP}$ (short: Rb/p53/PTEN) or $R26R^{LoxP/LoxP}$; $p53^{LoxP/LoxP}$; $PTEN^{LoxP/LoxP}$ (short: p53/PTEN). All mice were intercrossed from single mutant conditional knockout mice generated with the same strain ES cells (129 Ola). After generating double, triple or quadruple homozygous mouse lines, they were kept homozygous for all alleles and in-bred within the same colony. Further description of $PTEN^{LoxP/LoxP}$ mice is given in the report by Marino *et al* (2002); $Rb^{LoxP/LoxP}$ and $p53^{LoxP/LoxP}$ mice in the study by Marino *et al* (2000); and $R26R^{LoxP/LoxP}$ reporter mice are described in the study by Soriano (1999). Genotyping was carried out from tail DNA using standard PCR reactions. Primers are as published earlier: ROSA26-1, 2 3 (Soriano, 1999); LZ1 and LZ2 (Marino *et al*, 2000); Rb18, Rb19, p53a, p53b, p53c, p53–int10–fwd and p53–int10–rev (Marino *et al*, 2000), and PTEN A and S (Marino *et al*, 2002).

Animal were housed according to institutional and UK Home Office guidelines (Project licence 70/5540 and 70/6603).

Preparation and administration of adenovirus

The cre adenovirus vector was constructed and propagated essentially as described earlier (Akagi *et al*, 1997). Viral infection of SVZ cells was achieved by unilateral stereotaxic injections of 10^9 plaque-forming units Adeno-cre in phosphate buffered saline into anaesthetized mice placed in a Narishige SR 6N stereotaxic frame. The injection in relation to bregma was anterior 0 mm; lateral 0.5 mm and ventral 2.5 mm. Injections were administered with a Hamilton syringe 1701RN and 26G needle. GFAP-cre virus was constructed as described before (Merkle *et al*, 2007) and amplified as above.

Histological examination

Brains were fixed in 10% formalin, embedded in paraffin, cut into 3-μm sections and processed for haematoxylin-eosin (H&E) staining. Antibodies or antisera against the following antigens were used: GFAP (DAKO Z0334), NeuN (Chemicon MAB377), nestin (BD Pharmingen 556309); synaptophysin (Zymed 080130 prediluted); β-galactosidase (Abcam Ab616) BrdU (Abcam ab6326); GFP (Abcam ab290); MAP-2 (Chemicon MAB3418), Neurofilament 200 (Sigma N5389); EMA (DAKO M613); S-100 (DAKO Z0311); cytokeratin (MNF116, DAKO M0821).

All immunostaining was carried out using the automated Ventana Benchmark or Discovery (Ventana Medical Systems), or LEICA BondMax (LEICA Microsystems) automated staining apparatus following the manufacturer's guidelines, using biotinylated secondary antibodies and a horseradish peroxidase-conjugated streptavidin complex and diaminobenzidine as a chromogen. For immunofluorescent antigen detection, Vibratome sections of 30-μm thickness were sectioned from formalin-fixed, agarose-embedded and coronally oriented brains. Stains were carried out in multi-well plates, using Alexa-labelled antibodies (Molecular Probes) fluorochromes (488, 546 or 633 nm), and scanned on a ZEISS LSM510 META confocal laser scanning microscope.

Brain dissection, isolation, propagation and injection of neurospheres in vitro

Neurospheres were derived as previously described (Jacques *et al*, 1998). After dissociation into single cells using papain (Worthington, LS003124), they were infected with Adeno-Cre and Adeno-GFP (MOI of $\geqslant 5$). Cell growth was assayed 3 days after dissociation with the WST-1 reagent (Roche). Approximately 10–12 μl of the neurosphere suspension (containing approximately 1000 neurospheres or 1×10^6 cells) was injected into the left striatum of wild-type adult mice (bregma, 1.5 mm lateral, 2 mm deep.), using a 22-G needle attached to a 25-μl Hamilton syringe (RN1702).

Astrocyte culture and transplantation

Cells were derived from cortices of P2–P4 mice and cultured in DMEM high glucose, L-glutamine, 10% FCS, and 1% Pen/Strep, and infected with adenovirus (Adeno-cre, Adeno-GFP, MOI $\geqslant 5$) at approximately 80–90% confluence after passage 1 (p1) for 48 h. Infection efficacy was assessed in a β-gal assay. After passage 4 or 5, harvested cells were and injected into the striatum of adult wild-type mice (5×10^5 cells). Mice were killed at time points as indicated in Supplementary Table S3 and brains were processed as described above. Astrocyte growth rate was determined using a WST-1 assay.

Using modified culture conditions that were more similar to neurosphere growth, astrocytes were grown as floating sphere ('astrospheres'). For this experiment, we used *in vitro*-recombined Rb/p53 astrocytes, grown as adherent astrocytes until passage (P) 8. At P9, 1×10^6 astrocytes were plated into a 10cm dish containing NS medium as cited above (Jacques *et al*, 1998). They were grown as free-floating NS-like aggregates and were expanded to P12. They were split after the same amount of time as neurospheres, that is, after 12 days. For transplantation of astrospheres, we used the same protocol as for neurospheres.

PCR analysis of recombination

PCR analysis of Cre-mediated recombination was performed on genomic DNA extracted from different tumours or from adjacent normal brain tissue, microdissected from paraffin sections. PCR amplification was done with primers Rb212, Rb18 and Rb19E (Marino *et al*, 2000) yielding the following PCR products: 283 bp (unrecombined *RbLoxP* allele), 260 bp (recombined *Rb*D*19* allele) and 235 bp (wild type *Rb* allele) (Vooijs *et al*, 1998). p53 recombination

was assayed with p53-int1-fwd and p53-int10-rev yielding a 612-bp product (Marino *et al*, 2000).

TaqMan analysis of Rb pathway transcripts

TaqMan PCR was performed using commercially available primer/probe sets for genes as indicated. The C_t values were obtained from the data using Applied Biosystem Software SDS 1.3 automatic settings and ΔC_t was calculated by subtracting the 18S C_t value from each gene's C_t value. From these values, ΔC_t (gene)/ΔC_t (actin) ± s.d. was calculated. The graph displays average ± s.d. value of each group's ΔC_t. Two-way ANOVA with Bonferroni correction was used to calculate the significance of differences in gene expression between groups. GraphPad Prism 5.0 was used for performing the statistical analysis and generating the graphical output.

Supplementary data

Supplementary data are available at *The EMBO Journal* Online (http://www.embojournal.org).

Acknowledgements

We thank Dr Juan-Pedro Martinez-Barbera and Dr Jonathan Ham for their helpful comments on the paper. This study is supported by funds from the Samantha Dickson Brain Tumour Trust, The Brain Research Trust UK and Ali's Dream Charitable Foundation. TSJ is the recipient of an ICH/GOSH Clinician Scientist Award. AS was supported by a Brain Research Trust PhD Studentship and NH is a Brain Research Trust Senior Research Fellow. This study is also supported by NIH grant HD-32116 and by the Sandler Family Supporting Foundation. ZM was supported by the Carlos Baldoceda Foundation and UCSF Krevans Fellowship.

Conflict of interest

The authors declare that they have no conflict of interest.

References

Akagi K, Sandig V, Vooijs M, Van der Valk M, Giovannini M, Strauss M, Berns A (1997) Cre-mediated somatic site-specific recombination in mice. *Nucleic Acids Res* **25:** 1766–1773

Alcantara Llaguno S, Chen J, Kwon CH, Jackson EL, Li Y, Burns DK, Alvarez-Buylla A, Parada LF (2009) Malignant astrocytomas originate from neural stem/progenitor cells in a somatic tumor suppressor mouse model. *Cancer Cell* **15:** 45–56

Alvarez-Buylla A, Kohwi M, Nguyen TM, Merkle FT (2008) The heterogeneity of adult neural stem cells and the emerging complexity of their niche. *Cold Spring Harb Symp Quant Biol* **73:** 357–365

Alvarez-Buylla A, Temple S (1998) Stem cells in the developing and adult nervous system. *J Neurobiol* **36:** 105–110

Bachoo RM, Maher EA, Ligon KL, Sharpless NE, Chan SS, You MJ, Tang Y, DeFrances J, Stover E, Weissleder R, Rowitch DH, Louis DN, DePinho RA (2002) Epidermal growth factor receptor and Ink4a/Arf: convergent mechanisms governing terminal differentiation and transformation along the neural stem cell to astrocyte axis. *Cancer Cell* **1:** 269–277

Blouw B, Song H, Tihan T, Bosze J, Ferrara N, Gerber HP, Johnson RS, Bergers G (2003) The hypoxic response of tumors is dependent on their microenvironment. *Cancer Cell* **4:** 133–146

Bruggeman SW, Hulsman D, Tanger E, Buckle T, Blom M, Zevenhoven J, van Tellingen O, van Lohuizen M (2007) Bmi1 controls tumor development in an Ink4a/Arf-independent manner in a mouse model for glioma. *Cancer Cell* **12:** 328–341

Collins VP (2002) Cellular mechanisms targeted during astrocytoma progression. *Cancer Lett* **188:** 1–7

Conover JC, Doetsch F, Garcia-Verdugo JM, Gale NW, Yancopoulos GD, Alvarez-Buylla A (2000) Disruption of Eph/ephrin signaling affects migration and proliferation in the adult subventricular zone. *Nat Neurosci* **3:** 1091–1097

Ding H, Roncari L, Shannon P, Wu X, Lau N, Karaskova J, Gutmann DH, Squire JA, Nagy A, Guha A (2001) Astrocyte-specific expression of activated p21-ras results in malignant astrocytoma formation in a transgenic mouse model of human gliomas. *Cancer Res* **61:** 3826–3836

Doetsch F, Caille I, Lim DA, Garcia-Verdugo JM, Alvarez-Buylla A (1999) Subventricular zone astrocytes are neural stem cells in the adult mammalian brain. *Cell* **97:** 703–716

Doetsch F, Petreanu L, Caille I, Garcia-Verdugo JM, Alvarez-Buylla A (2002) EGF converts transit-amplifying neurogenic precursors in the adult brain into multipotent stem cells. *Neuron* **36:** 1021–1034

Fidler IJ (2003) The pathogenesis of cancer metastasis: the 'seed and soil' hypothesis revisited. *Nat Rev Cancer* **3:** 453–458

Forni PE, Scuoppo C, Imayoshi I, Taulli R, Dastru W, Sala V, Betz UA, Muzzi P, Martinuzzi D, Vercelli AE, Kageyama R, Ponzetto C (2006) High levels of Cre expression in neuronal progenitors cause defects in brain development leading to microencephaly and hydrocephaly. *J Neurosci* **26:** 9593–9602

Holland EC (2001) Gliomagenesis: genetic alterations and mouse models. *Nat Rev Genet* **2:** 120–129

Holland EC, Celestino J, Dai C, Schaefer L, Sawaya RE, Fuller GN (2000) Combined activation of Ras and Akt in neural progenitors induces glioblastoma formation in mice. *Nat Genet* **25:** 55–57

Holland EC, Hively WP, Gallo V, Varmus HE (1998) Modeling mutations in the G1 arrest pathway in human gliomas: overexpression of CDK4 but not loss of INK4a-ARF induces hyperploidy in cultured mouse astrocytes. *Genes Dev* **12:** 3644–3649

Jackson EL, Garcia-Verdugo JM, Gil-Perotin S, Roy M, Quinones-Hinojosa A, VandenBerg S, Alvarez-Buylla A (2006) PDGFR alpha-positive B cells are neural stem cells in the adult SVZ that form glioma-like growths in response to increased PDGF signaling. *Neuron* **51:** 187–199

Jacques TS, Relvas JB, Nishimura S, Pytela R, Edwards GM, Streuli CH, ffrench-Constant C (1998) Neural precursor cell chain migration and division are regulated through different beta1 integrins. *Development* **125:** 3167–3177

Jacques TS, Skepper JN, Navaratnam V (1999) Fibroblast growth factor-1 improves the survival and regeneration of rat vagal preganglionic neurones following axon injury. *Neurosci Lett* **276:** 197–200

Kessler JD, Hasegawa H, Brun SN, Yang ZJ, Dutton JW, Wang F, Wechsler-Reya RJ (2009) N-myc alters the fate of preneoplastic cells in a mouse model of medulloblastoma. *Genes Dev* **23:** 157–170

Kwon CH, Zhao D, Chen J, Alcantara S, Li Y, Burns DK, Mason RP, Lee EY, Wu H, Parada LF (2008) Pten haploinsufficiency accelerates formation of high-grade astrocytomas. *Cancer Res* **68:** 3286–3294

Loonstra A, Vooijs M, Beverloo HB, Allak BA, van Drunen E, Kanaar R, Berns A, Jonkers J (2001) Growth inhibition and DNA damage induced by Cre recombinase in mammalian cells. *Proc Natl Acad Sci USA* **98:** 9209–9214

Louis DN, Ohgaki H, Wiestler OD, Cavenee WK (eds) (2007) *WHO Classification of Tumours of the Central Nervous System*. Lyon, France: IARC Press

Marino S, Krimpenfort P, Leung C, van der Korput HA, Trapman J, Camenisch I, Berns A, Brandner S (2002) PTEN is essential for cell migration but not for fate determination and tumourigenesis in the cerebellum. *Development* **129:** 3513–3522

Marino S, Vooijs M, van Der Gulden H, Jonkers J, Berns A (2000) Induction of medulloblastomas in p53-null mutant mice by somatic inactivation of Rb in the external granular layer cells of the cerebellum. *Genes Dev* **14:** 994–1004

Marumoto T, Tashiro A, Friedmann-Morvinski D, Scadeng M, Soda Y, Gage FH, Verma IM (2009) Development of a novel mouse glioma model using lentiviral vectors. *Nat Med* **15:** 110–116

Merkle FT, Mirzadeh Z, Alvarez-Buylla A (2007) Mosaic organization of neural stem cells in the adult brain. *Science* **317:** 381–384

Naiche LA, Papaioannou VE (2007) Cre activity causes widespread apoptosis and lethal anemia during embryonic development. *Genesis* **45:** 768–775

Oliver TG, Wechsler-Reya RJ (2004) Getting at the root and stem of brain tumors. *Neuron* **42:** 885–888

Rietze RL, Reynolds BA (2006) Neural stem cell isolation and characterization. *Methods Enzymol* **419:** 3–23

Sanai N, Alvarez-Buylla A, Berger MS (2005) Neural stem cells and the origin of gliomas. *N Engl J Med* **353:** 811–822

Sherr CJ, Weber JD (2000) The ARF/p53 pathway. *Curr Opin Genet Dev* **10:** 94–99

Sonoda Y, Ozawa T, Aldape KD, Deen DF, Berger MS, Pieper RO (2001) Akt pathway activation converts anaplastic astrocytoma to glioblastoma multiforme in a human astrocyte model of glioma. *Cancer Res* **61:** 6674–6678

Soriano P (1999) Generalized lacZ expression with the ROSA26 Cre reporter strain. *Nat Genet* **21:** 70–71

Stiles CD, Rowitch DH (2008) Glioma stem cells: a midterm exam. *Neuron* **58:** 832–846

Tao W, Levine AJ (1999) P19(ARF) stabilizes p53 by blocking nucleo-cytoplasmic shuttling of Mdm2. *Proc Natl Acad Sci USA* **96:** 6937–6941

Uhrbom L, Kastemar M, Johansson FK, Westermark B, Holland EC (2005) Cell type-specific tumor suppression by Ink4a and Arf in Kras-induced mouse gliomagenesis. *Cancer Res* **65:** 2065–2069

Vooijs M, Jonkers J, Berns A (2001) A highly efficient ligand-regulated Cre recombinase mouse line shows that LoxP recombination is position dependent. *EMBO Rep* **2:** 292–297

Vooijs M, van der Valk M, te Riele H, Berns A (1998) Flp-mediated tissue-specific inactivation of the retinoblastoma tumor suppressor gene in the mouse. *Oncogene* **17:** 1–12

Wang Y, Yang J, Zheng H, Tomasek GJ, Zhang P, McKeever PE, Lee EY, Zhu Y (2009) Expression of mutant p53 proteins implicates a lineage relationship between neural stem cells and malignant astrocytic glioma in a murine model. *Cancer Cell* **15:** 514–526

Xiao A, Wu H, Pandolfi PP, Louis DN, Van Dyke T (2002) Astrocyte inactivation of the pRb pathway predisposes mice to malignant astrocytoma development that is accelerated by PTEN mutation. *Cancer Cell* **1:** 157–168

Xiao A, Yin C, Yang C, Di Cristofano A, Pandolfi PP, Van Dyke T (2005) Somatic induction of Pten loss in a preclinical astrocytoma model reveals major roles in disease progression and avenues for target discovery and validation. *Cancer Res* **65:** 5172–5180

Yang ZJ, Ellis T, Markant SL, Read TA, Kessler JD, Bourboulas M, Schuller U, Machold R, Fishell G, Rowitch DH, Wainwright BJ, Wechsler-Reya RJ (2008) Medulloblastoma can be initiated by deletion of Patched in lineage-restricted progenitors or stem cells. *Cancer Cell* **14:** 135–145

Zheng H, Ying H, Yan H, Kimmelman AC, Hiller DJ, Chen AJ, Perry SR, Tonon G, Chu GC, Ding Z, Stommel JM, Dunn KL, Wiedemeyer R, You MJ, Brennan C, Wang YA, Ligon KL, Wong WH, Chin L, DePinho RA (2008) p53 and Pten control neural and glioma stem/progenitor cell renewal and differentiation. *Nature* **455:** 1129–1133

Zhu Y, Guignard F, Zhao D, Liu L, Burns DK, Mason RP, Messing A, Parada LF (2005a) Early inactivation of p53 tumor suppressor gene cooperating with NF1 loss induces malignant astrocytoma. *Cancer Cell* **8:** 119–130

Zhu Y, Harada T, Liu L, Lush ME, Guignard F, Harada C, Burns DK, Bajenaru ML, Gutmann DH, Parada LF (2005b) Inactivation of NF1 in CNS causes increased glial progenitor proliferation and optic glioma formation. *Development* **132:** 5577–5588